7-2020

# Resonance Raman Spectroscopic Studies of Peroxo and Hydroperoxo Intermediates in Lauric Acid (LA)-Bound Cytochrome P450 119

Remigio Usai
*Marquette University*

Daniel Kaluka
*Marquette University*

Piotr J. Mak
*Marquette University*, piotr.mak@marquette.edu

Yilin Liu
*Marquette University*

James R. Kincaid
*Marquette University*, james.kincaid@marquette.edu

*Journal of Inorganic Biochemistry*, Vol. 208, (2020, July): 111084. DOI. 

# Resonance Raman Spectroscopic Studies of Peroxo and Hydroperoxo Intermediates in Lauric Acid (LA)-Bound Cytochrome P450 119

Remigio Usai
Department of Chemistry, Marquette University, Milwaukee, WI
Daniel Kaluka
Taylor University, Department of Chemistry and Biochemistry, Upland, IN
Department of Chemistry, Marquette University, Milwaukee, WI
Piotr J. Mak
St. Louis University, Department of Chemistry, St. Louis, MO
Department of Chemistry, Marquette University, Milwaukee, WI
Yilin Liu
Department of Chemistry, Marquette University, Milwaukee, WI
James R. Kincaid
Department of Chemistry, Marquette University, Milwaukee, WI

## Abstract

Cytochromes P450 bind and cleave dioxygen to generate a potent intermediate compound I, capable of hydroxylating inert hydrocarbon substrates. Cytochrome P450 119, a bacterial cytochrome P450 that serves as a good model system for the study of the intermediate states in the P450 catalytic cycle. CYP119 is found in high temperature and sulfur rich environments. Though the natural substrate and redox partner are still unknown, a potential application of such thermophilic P450s is utilizing them as biocatalysts in biotechnological industry; e.g., the synthesis of organic compounds otherwise requiring hostile environments like extremes of pH or temperature. In the present work the oxygenated complex of this enzyme bound to lauric acid, a surrogate substrate known to have a good binding affinity, was studied by a combination of cryoradiolysis and resonance Raman spectroscopy, to trap and characterize active site structures of the key fleeting enzymatic intermediates, including the peroxo and hydroperoxo species.

## Graphical abstract

CYP119 is a thermophilic Cytochrome P450 which cleaves dioxygen to generate the potent intermediate, compound I, which is capable of hydroxylating hydrocarbon substrates. Here cryoradiolysis of the oxygenated complex, was employed to generate and trap the precursor peroxo and hydroperoxo enzymatic intermediates, which were characterized by resonance Raman spectroscopy.

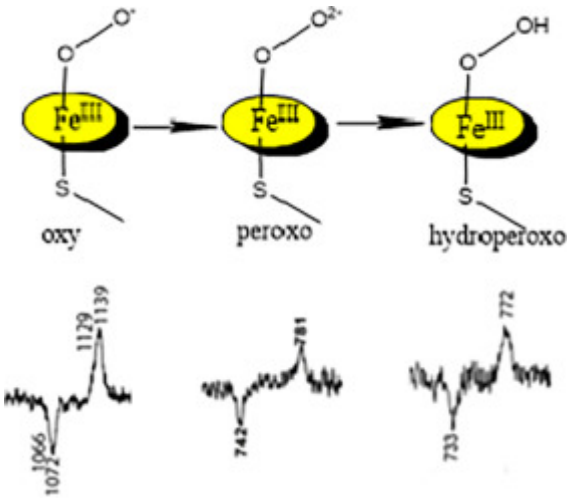


## Keywords

Heme proteins, Cytochrome P450, CYP119, Raman, Cryoradiolysis, Intermediates

## 1. Introduction

The Cytochrome P450s are among nature's most versatile and ubiquitous enzymes because of their extraordinary ability to perform highly regio- and stereo-selective oxidation reactions on a wide variety of compounds including alkanes, fatty acids, terpenes, steroids, detoxification of carcinogens, pesticides and other pharmaceuticals [[1], [2], [3], [4]]. Using molecular oxygen and reducing equivalents supplied by redox partner proteins, cytochromes P450 can efficiently catalyze difficult reactions known to occur in biological systems, including hydroxylation of inert hydrocarbons through a concerted reaction mechanism [5]. As seen in Scheme 1, the substrate binds to the low spin ferric six coordinate resting state [species 1] forming a 5-coordinate high spin complex [species 2]. One electron reduction and subsequent oxygen binding forms the oxygenated complex [species 4]. Another electron reduction forms the peroxo intermediate [species 5] which is protonated to form a hydroperoxo intermediate [species 6], with another protonation step leading to O—O bond cleavage and

formation of compound I [species 7]. It is very difficult to trap the peroxo and hydroperoxo intermediates, owing to rapid proton transfer and subsequent O—O bond cleavage following reduction to the $O_2$-complex. However, a useful approach to study these species is cryoradiolysis, introduced by Symons [6,7]. Here the relatively more stable oxygenated complex is cryotrapped (77 K) and subjected to radiolysis by a $^{60}Co$ γ-ray source; while radiolytically generated electrons can migrate at 77 K, proton migration is much more restricted. Indeed, this approach has been utilized and refined by Hoffman and others to study a variety of heme proteins [[8], [9], [10], [11], [12], [13], [14], [15]].

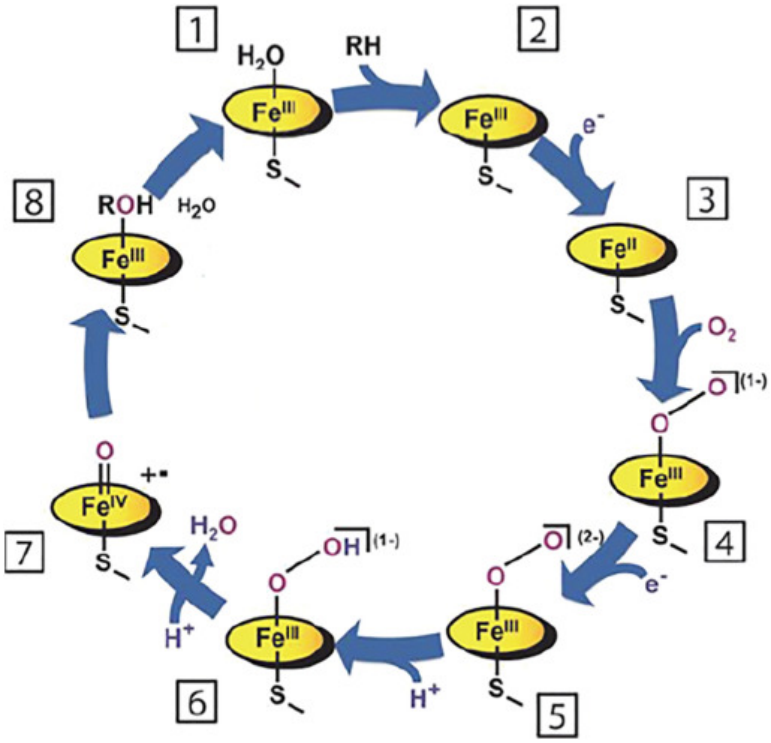


Scheme 1. Cytochrome P450 catalytic cycle [2,30].

The bacterial enzyme, Cytochrome P450 119 (CYP119), is an acidothermophilic P450 from *Sulfolobus solfataricus*, which is found in sulfur rich environments in hot springs [[16], [17], [18], [19], [20], [21]]. This enzyme exhibits high thermal stability, with its optimal growth occurring near 85 °C [16]. The enzyme is easily expressed in *E. coli* [18,20,22], but its natural substrate and redox partners are still unknown [16,19]. Previous studies have shown that this enzyme hydroxylates surrogate substrates including, lauric acid (LA) [19], styrene [23], palmitic acid [24,25], and caprylic acid [24,25]. The hydroxylation reaction of lauric acid catalyzed by CYP119 yields ~70% of 11-hydroxylauric acid (ω-1), ~22% of 10-hydroxylauric acid (ω-2), 7% 12-hydroxylauric acid (ω) and 1% 9-hydroxylauric acid (ω-3), as shown in Scheme 2 below.

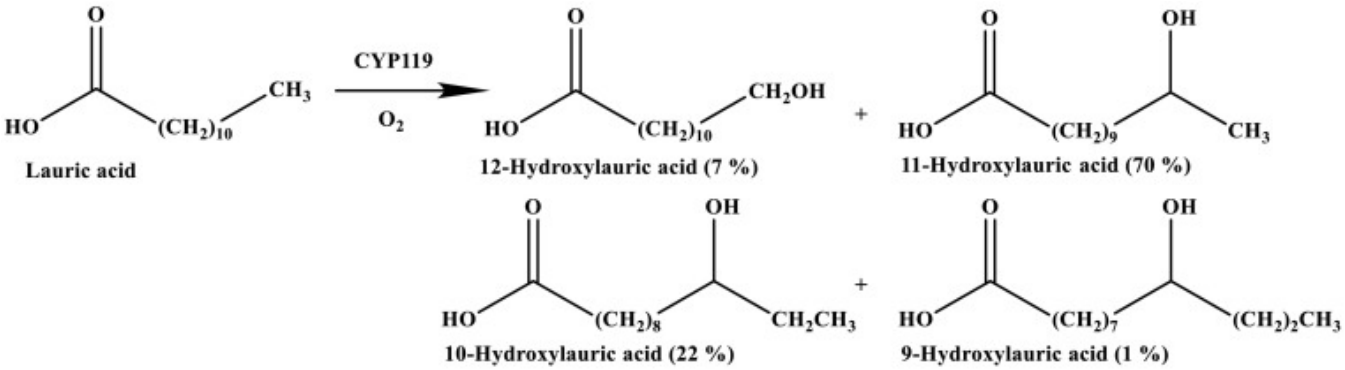


Scheme 2. $O_2$ reaction of Lauric acid (LA) catalyzed by CYP119 showing the major ω-hydroxylation products ω (12-hydroxylauric acid), ω-1 (11-hydroxylauric acid), ω-2 (10-hydroxylauric acid) and ω-3 (9-hydroxylauric acid) [20].

As clearly outlined in reviews by Terner and others [[26], [27], [28], [29], [30]], resonance Raman (RR) spectroscopy is an attractive probe of the intermediates encountered in the P450 cycle, being capable of interrogating both the heme macrocycle and the iron-ligand fragments. Following early attempts to acquire the RR spectrum of Compound I intermediates of peroxidases, which met with difficulties owing to photosensitivity with violet probe beams [26,27], the first apparently valid spectrum was reported using near UV excitation by Terner and coworkers [31], as later confirmed by others.[32] Coupling RR spectroscopy with cryoradiolysis has proven to be particularly effective in trapping and characterizing the peroxo- and hydroperoxo- intermediates [[11], [12], [13], [14], [15],30,33]. In this present study we report high quality RR data for the LA bound CYP119 oxygenated complexes before and after cryoradiolysis to generate, trap and structurally characterize key catalytic intermediates, including the oxy-, peroxo- and hydroperoxo- forms.

# 2. Materials and methods

## 2.1. Materials

The plasmid encoding the CYP119 gene was kindly provided by Dr. Stephen G. Sligar of the University of Illinois at Urbana Champaign. Competent BL21 *E. coli* cells were purchased from Biolabs. CYP119 was expressed and purified as previously published [18]. The samples used had a Reinheitszahl ratio (Rz) value ($A_{415}/A_{280}$) > 1.5, the published value for the pure enzyme [34]. The protein concentrations were determined by UV–visible absorption spectroscopy using the mM absorptivity value of 104 $mM^{-1}$ $cm^{-1}$ at 415 nm for the ferric, substrate-free enzyme [18]. Glycerol solutions for making cryotrapped oxygenated complexes were purified, and checked for residual fluorescence with resonance Raman spectroscopy as previously described [35]. Deuterated glycerol[$(OD)_3$, 95%] was made by mixing commercial glycerol (boiling point 182 °C) [35] with a 20-fold molar excess of deuterium oxide, then refluxed at 100 °C for 30 min. The temperature was increased to 130 °C to distil the $H_2O/D_2O$. The product remaining after distillation was characterized by Raman spectroscopy and spectrum compared with that of commercial $D_3$- glycerol [[35], [36], [37]], and the boiling point of $d_3$-glycerol was 182 °C (Literature value of boiling point for $D_3$-glycerol is 182 °C (Cambridge isotopes)).

## 2.2. Methods

### 2.2.1. Protein preparation

CYP119 was transformed, expressed and purified according to previously published procedures [18], with minor modifications. Briefly, CYP119 was transformed in BL21 cells followed by growing in LB broth with 100 mg/L ampicillin overnight at 37 °C and 250 rpm. A 1% starter culture was inoculated and expressed in 2× YT medium supplemented with 100 mg/L ampicillin for 20 h at 37 °C and 250 rpm. Cells were harvested by centrifugation at

9148 ×*g* for 15 min at 4 °C and stored in a − 80 °C freezer. To isolate protein, cells were thawed and resuspended in 4 volumes (4 mL/g cell paste) of lysis buffer (50 mM Tris/HCl pH 8.0, 1 mM EDTA, 4 mg/mL lysozyme, 16 U/mL DNase, 4 U/mL RNase) and stirred gently at 4 °C, followed by centrifugation at 47850 ×*g* for 1 h. The supernatant was incubated at 75 °C for 15 min followed by centrifugation at 7656 ×*g* for 30 min to remove the unwanted denatured bacterial proteins [18]. The supernatant was saturated with 40% ammonium sulfate and shaken gently at 4 °C for 30 min followed by centrifugation at 7656 ×*g* for 30 min. The supernatant was saturated to 60% ammonium sulfate and shaken gently at 4 °C for 30 min followed by centrifugation at 7656 ×*g* for 30 min. The pellet was resuspended in a minimum volume (about 10 mL) of 10 mM phosphate buffer, pH 7.2 and stored in −80 °C freezer until needed for the next purification step.

The protein was further purified on a Bio-Rad P100 gel filtration column equilibrated with 10 mM phosphate buffer pH 7.2. Fractions with Rz values >0.5 were combined and loaded onto a DEAE 53 column equilibrated with 10 mM phosphate buffer, pH 7.2, washed thoroughly with 6 column volumes of this 10 mM phosphate buffer, pH 7. The column was then eluted using a 10–100 mM gradient in phosphate buffer at pH 7.2. Fractions with Rz values >1.1 were combined and further purified by loading onto another P100 gel filtration column equilibrated with 10 mM PB pH 7.2 [38]. Fractions with Rz > 1.5 were combined, concentrated and stored in a − 80 °C freezer and later used for the studies described below.

### 2.2.2. Electronic absorption spectrophotometry

Electronic absorption spectrophotometric measurements were performed using a Hewlett-Packard, Model 8452 Diode Array Spectrometer.

### 2.2.3. Resonance Raman spectroscopy

Final concentrations of all samples of oxygenated complexes were 200 μM CYP119 in 100 mM phosphate buffer (PB), pH 8.0, containing 0.30 M NaCl and 30% glycerol. Samples of oxygenated CYP119 were prepared on a vacuum line by adding dioxygen gas to 30% glycerol/buffer solutions of the (ferrous) enzyme in 5 mm NMR tubes. The ferrous CYP119 was obtained by adding 1.5–2.0 equivalents of sodium dithionite solution via a syringe through a septum to a ferric protein that was under an argon atmosphere [39]. The ferrousCYP119 solution was cooled to −20 °C and oxygenated by adding oxygen gas and agitated by rapidly mixing manually for 3–5 s and then quickly frozen in liquid nitrogen [21,39]. RR spectra were obtained using a Spec 1269 spectrometer equipped with a Spec-10 LN (liquid nitrogen cooled) detector (Princeton Instruments, NJ). The sample-containing NMR tubes were positioned into a homemade double-walled quartz low temperature Dewar filled with liquid nitrogen. The sample tubes were spun to avoid local heating. The excitation line employed for oxy samples was 413.1 nm (Coherent Sabre Kr ion laser); for peroxo and hydroperoxo samples the 441.6 nm line was used (Kimmon Model IK4153RC He:Cd laser). Fenchone spectra were used to calibrate all spectra, which were processed using Grams 32/AI (Galactic Industries, Salem, NH). Rayleigh scattering was removed by use of an appropriate Notch filter from Kaiser Optical (HNF-413-1.0 for 413.1 nm excitation line and CNPF-441.6-1,0 for 441.6 nm excitation line). The NMR tube containing the sample was spun and the RR spectra collected at liquid $N_2$ temperature using 180° (back scattering) geometry in combination with a cylindrical lens, which focusses the laser beam in a line image on the sample to minimize local heating. In acquiring RR spectra of the frozen samples, the laser power at the sample was also minimized to prevent sample heating, which in the case of bacterial P450s can sometimes lead to heat-induced proton transfer; i.e., attempts to measure the peroxo-intermediate were conducted with much care to minimize generation of the hydroperoxo- intermediate. For all RR measurements, the slit width was set at 150 μm; with the 1200 g/mm grating being used, the linear reciprocal dispersion is 0.655 nm/mm near 400 nm, corresponding to 0.46 $cm^{-1}$/pixel [36].

### 2.2.4. Irradiation procedure

The cryoradiolytic reduction of CYP119 samples was done by exposing the samples to 3.5 Mrad of γ-irradiation from a $^{60}$Co source at the Notre Dame Radiation Laboratory (University of Notre Dame, South bend, IN), as described in previous studies [9,10,39]. During the γ-ray irradiation procedure, the samples were contained in a modified Dewar vessel and continuously immersed in the liquid nitrogen at all times during and following the irradiation procedure in the $^{60}$Co source chamber.

### 2.2.5. Deconvolution procedure

Deconvolution procedures in the region of 1000–1200 cm$^{-1}$ for the resonance Raman spectra of oxygenated CYP119 with LA bound were conducted using Grams 32/A1 programs (Galactic Industries Co., Salem, NH). Briefly, a 50% Lorentzian/Gaussian band shape for all bands was assumed and fixed, because using this combination of functions, the best fit to the band profiles in the Raman spectra was obtained. The detailed strategy for the fitting procedure is described elsewhere [40,41].

## 3. Results and discussion

### 3.1. RR spectra of the dioxygen adduct of CYP119 with LA bound

The formation of oxy ferrous complex of LA bound CYP119 was confirmed by RR spectroscopy at 77 K. The medium frequency spectra which allow simultaneous observation of the *ν*(Fe–O) and ν(O–O) regions are shown in Fig. 1 for the LA-bound samples. The spectra were acquired for $^{16}O_2$ and $^{18}O_2$ samples in $H_2O$ buffer (A and B, respectively), and for $^{16}O_2$ and $^{18}O_2$ samples in $D_2O$ buffer solutions (C and D, respectively). Furthermore, the $^{16}O_2$ - $^{18}O_2$ difference traces were generated and are shown at the bottom of Fig. 1. To get better insight into the ν(O–O) envelope, careful deconvolution was performed using 50/50% Gaussian/Lorentzian functions of 11.0 cm$^{-1}$ ± 0.5 cm$^{-1}$ bandwidth, and the results of this band fitting are shown in Fig. 2. Inspection of Fig. 2 clearly indicates that the asymmetric envelope of O–O bands can be deconvoluted into two modes, a lower frequency mode at 1130 cm$^{-1}$ that is much less populated and a dominant higher frequency mode at 1139 cm$^{-1}$. These modes exhibit $^{16/18}$O shifts of 66 and 65 cm$^{-1}$, respectively, as expected for an O–O harmonic oscillator [42]. Inspection of the difference pattern in the $D_2O$ buffer (trace B of Fig. 2) indicates that the lower frequency mode is H/D sensitive and is upshifted by 2 cm$^{-1}$ in $D_2O$ buffer. It is noted that these types of rR spectroscopic patterns are reflective of H-bonding interactions observed in careful studies of cytochrome P450 model compounds [43,44], where the *ν*($^{16}$O–$^{16}$O) mode for the oxy complex of a “picket fence” model, with its hydrophobic oxygen binding pocket, is observed near 1147 cm$^{-1}$, [43] while this mode was observed near 1138 cm$^{-1}$ for a P450 model of a super-structured heme possessing H-bonding hydroxide groups in its oxygen binding pocket [44]. Furthermore, for this latter model, the ν($^{16}$O–$^{16}$O) was observed to shift up by 2 cm$^{-1}$ when the –OH groups were replaced with -OD groups [44].

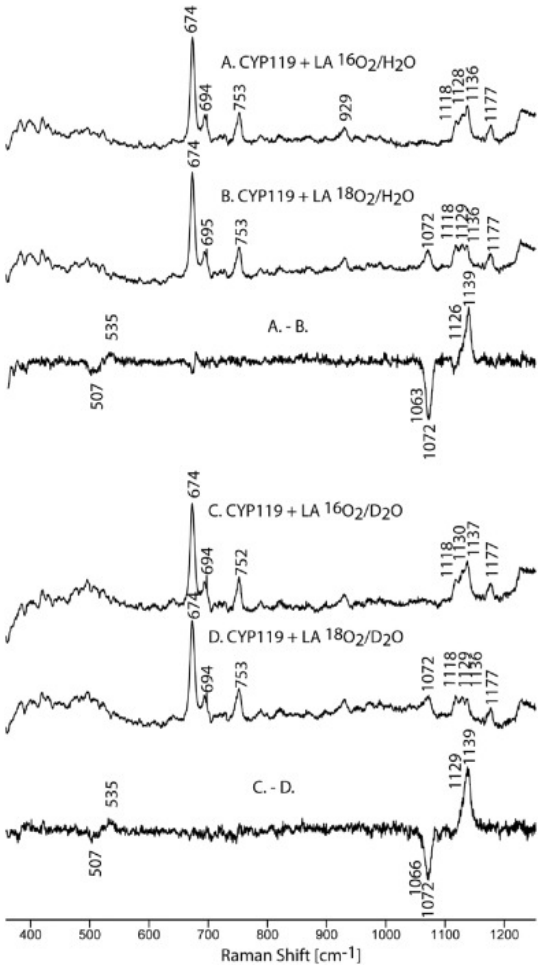


Fig. 1. Resonance Raman spectra of oxy CYP119 with LA; A) $^{16}O_2/H_2O$, B) $^{18}O_2/H_2O$, C) $^{16}O_2/D_2O$, D) $^{18}O_2/D_2O$, and their difference traces. Spectra were measured with 413.1 nm excitation line at 77 K, the total collection time was 5 h for each spectrum and ~ 1.4 mW power was used.

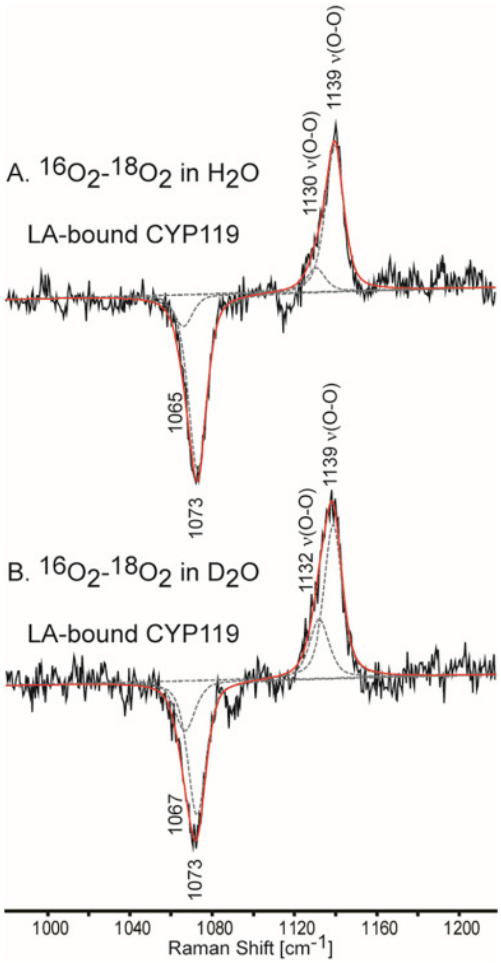


Fig. 2. The deconvoluted $^{16}O_2$- $^{18}O_2$ traces in $H_2O$ (A) and $D_2O$ (B) buffers for the LA-bound oxyCYP119.

Returning attention to the current study of CYP119, the frequency of the 1139 cm$^{-1}$ mode and its lack of H/D sensitivity indicate that this Fe-O-O conformer doesn't participate in any substantial H-bonding interactions. On the other hand, the 9 cm$^{-1}$ downshift of the weaker lower frequency mode and its H/D sensitivity clearly indicate that this less populated conformer is H-bonded with some active site H-bond donor. Since the substrate contains no H-bond donors, the potential H-bond donors are acid/alcohol pair E212/T213 for CYP119 or more likely water molecules. Consistent with this interpretation, it is noted that crystallographic data show that a distal pocket water molecule lies close to the iron and also interacts with the highly conserved Thr 213 [34]. It is noted that these RR data observed for CYP119 are similar to those CYP101 and its D251N mutant, where H-bonded and non-H bonded Fe-O-O conformers were also identified [14,45].

In the low-frequency region of the RR spectra, a feature assigned to the *ν*(Fe—O) stretching mode is seen at 535 cm$^{-1}$ (Fig. 1) and exhibits a 28 cm$^{-1}$ shift upon $^{18}O_2$ substitution and no H/D sensitivity. It is noted that while the ν(O—O) modes of the two conformers are isolated, apparently the corresponding ν(Fe—O) modes are sufficiently close in energy to prevent resolution. In any case, these ν(Fe—O) modes observed here are similar to those seen for other oxygenated P450s; i.e., 537 cm$^{-1}$ in D251N mutant and ~ 540 cm$^{-1}$ in CYP101.

In summary, the oxy complex of the LA- bound sample of CYP119 was successfully prepared and characterized by RR spectroscopy. The careful deconvolution studies revealed that the dioxygen adduct possesses two Fe-O-O conformers, with an H-bonded form whose *ν*(O—O) appears 7 cm$^{-1}$ lower than that of the dominant non-H-bonded form, behavior also seen for oxy complexes of other cytochromes P450 [15,30]. It is noted that only one

feature associated with the ν(Fe—O) mode was observed at 534–535 $cm^{-1}$, possibly the result of two features having only small differences in inherent frequency.

## 3.2. Resonance Raman studies of cryoradiolytically reduced samples of oxyCYP119

In beginning the discussion of the spectroscopic data for the cryoreduced samples, it is important to note that some P450 enzymes apparently have very efficient proton delivery pathways, making it more difficult to trap the peroxo intermediate. For example, in the case of the bacterial enzyme, cytochrome P450cam (CYP101), the hydroperoxo-intermediate formed even at 77 K for the wild type enzyme, with the peroxo intermediate being observed only for the D251N mutant, which cripples the proton shuttle [14]. In the present work the oxygenated samples of CYP119 bound to LA were irradiated and handled according to previously published procedures [[9], [10], [11], [12], [13], [14]]. However, initial attempts, in this work and earlier [46], to measure the peroxo species, inadvertently generated the spectra of the hydroperoxo species. Later, more care was taken and multiple efforts were made using adequately low laser powers, or slightly defocused excitation laser, until RR spectra were acquired that were consistent with that for the peroxo intermediate. These acquired RR spectra of $^{16}O_2$ and $^{18}O_2$ samples in $H_2O$ and $D_2O$ buffers, as well as their difference traces are shown in Fig. 3, below. The *ν*(Fe—O) mode of the peroxo-CYP119 species produced by cryoradiolytic reduction of oxy-CYP119 was observed to occur at 547 $cm^{-1}$, exhibiting a 26 $cm^{-1}$ shift for the $^{18}O$ analogue, consistent with that expected for a Fe—O harmonic oscillator [42]. The ν(O—O) was observed at 781 $cm^{-1}$ and shifts down to 742 $cm^{-1}$ for the $^{18}O$ analogue, yielding a 39 $cm^{-1}$ downshift upon isotope substitution. There is no significant $H_2O/D_2O$ sensitivity for this feature, confirming its assignment as the *ν*(O—O) mode for the peroxo intermediate [14,47].

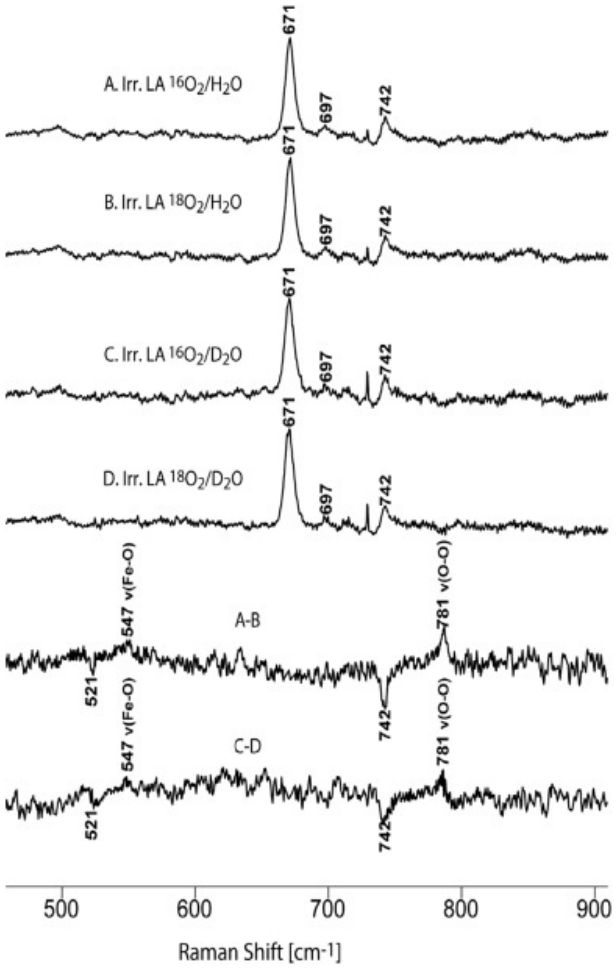

Fig. 3. Resonance Raman spectra of irradiated dioxygen adducts of LA bound CYP119 A) $^{16}O_2/H_2O$, B) $^{18}O_2/H_2O$, C) $^{16}O_2/D_2O$, D) $^{18}O_2/D_2O$, and their difference traces. Spectra were measured with 441.6 nm excitation line at 77 K, the total collection time was 6 h for each spectrum and ~ 1 mW power was used.

Fig. 4 shows RR data for oxy adducts of CYP119 bound with LA measured after irradiation at 77 K using the 441.6 nm excitation line. Here, relatively higher laser power, or possibly tighter laser focusing, apparently induced local heating on the frozen sample [48]. The acquired RR spectra exhibit an oxygen isotope sensitive mode at 772 $cm^{-1}$, shifting to 733 $cm^{-1}$ for the $^{18}O_2$ sample, along with a 5 $cm^{-1}$ downshift in $D_2O$ buffer; the frequency and H/D sensitivity permits confident assignment of this mode to the *ν*(O—O) stretching mode of the hydroperoxo intermediate. The corresponding ν(Fe—O) mode is seen at 569 $cm^{-1}$ and shifts by 27 $cm^{-1}$ upon $^{18}O_2$ substitution, possibly exhibiting a small H/D shift of ~1 $cm^{-1}$. The accuracy of the absolute frequencies is about ±1 $cm^{-1}$and it is noted that this is within the margin of error. This apparent strengthening of the Fe—O bond, with its ν(Fe—O) frequency of 569 $cm^{-1}$, as compared to the Fe—O bond of the peroxo intermediate (547 $cm^{-1}$) is consistent with the formation of the hydroperoxo form [14,47]. It is also noted that previously published EPR studies of irradiated oxy adducts of substrate-free CYP119, acquired after annealing at 150 K, showed formation of the hydroperoxo intermediate [21].

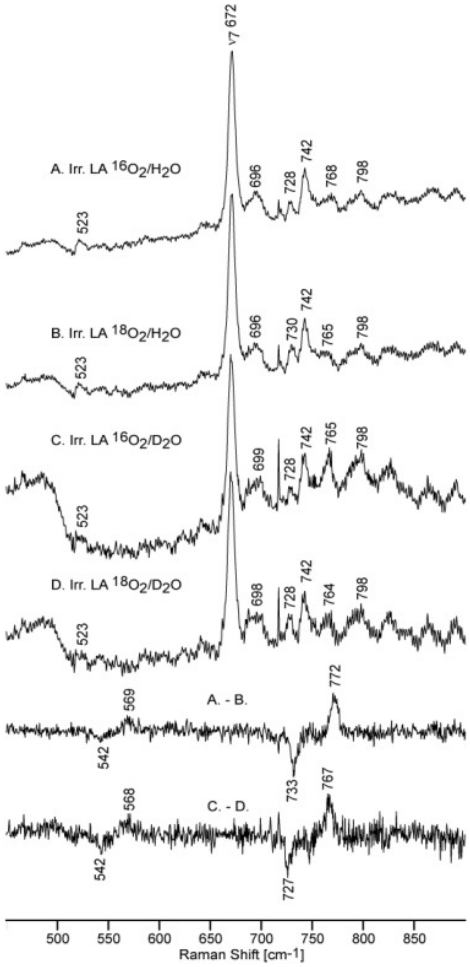


Fig. 4. Resonance Raman spectra of oxy CYP119 with LA after irradiation; A) $^{16}O_2/H_2O$, B) $^{18}O_2/H_2O$, C) $^{16}O_2/D_2O$, D) $^{18}O_2/D_2O$, and their difference traces. Total collection time was 6 h for each spectrum and ~ 1.4 mW laser power was used.

In summary of this section, Table 1 compares the data for peroxo- and hydroperoxo intermediates of CYP119 obtained in this work with similar data obtained previously on other cytochromes P450 (references in the Table 2). The data show that bacterial P450s (CYP101 and CYP119) exhibit rapid proton transfer, readily forming the hydroperoxo- intermediate, behavior consistent with their propensity to facilitate hydroxylase chemistry. On the other hand, the multifunctional P450, CYP17, whose peroxo- intermediate has been implicated in the mechanism for lyase activity via nucleophilic attack on a susceptible C20– carbonyl of OH– PREG [11,12], interestingly, shows no tendency to form the hydroperoxo-intermediate when OH PREG is bound, even when annealing to 165 K, behavior that has been ascribed to the enhanced nucleophilicity, and therefore lyase activity of the peroxo-intermediate, owing to a particular H-bonding interaction of the 17-OH group with the proximal oxygen ($O_p$) of the Fe-$O_p$-$O_t$ fragment [12].

Table 1. CYP 119 O—O and Fe—O stretching modes of cryoreduced oxy complexes relative to those observed other P450 enzymes.

| **Cytochrome** | | **ν(O—O) oxy ($cm^{-1}$)** | | ***ν*(O—O) peroxo- ($cm^{-1}$)** | | **ν(O—O) hydroperoxo- ($cm^{-1}$)** | | **ν(Fe—O) oxy ($cm^{-1}$)** | | **ν(Fe—O) peroxo- ($cm^{-1}$)** | | **ν(Fe—O) hydroperoxo- ($cm^{-1}$)** | |
|---|---|---|---|---|---|---|---|---|---|---|---|---|---|
| **Buffer (see cited references for details)** | | **$H_2O$** | **$D_2O$** | **$H_2O$** | **$D_2O$** | **$H_2O$** | **$D_2O$** | **$H_2O$** | **$D_2O$** | **$H_2O$** | **$D_2O$** | **$H_2O$** | **$D_2O$** |
| CYP119 | $^{16}O_2$ | 1139 | 1139 | 781[1] | 781[1] | 772 | 767 | 535 | 535 | 547 | 547 | 569 | 568 |
| this work | $^{18}O_2$ | 1072 | 1072 | 742[1] | 742[1] | 733 | 727 | 507 | 507 | 521 | 521 | 542 | 542 |
| | $^{16}O_2$ | 1130 | 1132 | | | | | | | | | | |
| | $^{18}O_2$ | 1065 | 1067 | | | | | | | | | | |
| CYP101 wild | $^{16}O_2$ | 1139 | 1139 | N.O. N.O. | N.O. | 799 | 796 | 546 | 546 | N.O. | N.O. | 559 | 556 |
| type [43,45] | $^{18}O_2$ | 1073 | 1073 | | N.O. | 759 | 755 | 515 | 515 | N.O. | N.O. | 532 | 528 |
| | $^{16}O_2$ | 1131 | | | | | | | | | | | |
| | $^{18}O_2$ | 1066 | | | | | | | | | | | |
| CYP101 | $^{16}O_2$ | 1136 | 1136 | 792 | 792 | 774 | 770 | 537 | 537 | 553 | 553 | 564 | 562 |
| (D251N) mutant | $^{18}O_2$ | 1070 | 1070 | 754 | 754 | 737 | 734 | 507 | 507 | 526 | 526 | 536 | 534 |
| [14,45] | $^{16}O_2$ | 1125 | 1127 | | | | | | | | | | |
| | $^{18}O_2$ | 1060 | 1062 | | | | | | | | | | |
| CYP17A1 | $^{16}O_2$ | 1140 | 1140 | N.O. | N.O. | 772 | 768 | 536 | 536 | N.O. N.O. | N.O. | 575 | 572 |
| Prog [11,12] | $^{18}O_2$ | 1074 | 1074 | N.O. | N.O. | 735 | 731 | 508 | 508 | | N.O. | 549 | 546 |
| CYP17A1 | $^{16}O_2$ | 1131 | 1133 | 790 | 790 | 771 | 768 | 542 | 542 | 562 | 561 | 576 | 574 |
| 17-OH Prog | $^{18}O_2$ | 1066 | 1068 | 753 | 753 | 734 | 730 | 513 | 513 | 536 | 536 | 550 | 548 |
| [11,12] | | | | | | | | | | | | | |
| CYP17A1 | $^{16}O_2$ | 1140 | 1140 | 802 | 802 | 775 | 770 | 535 | 535 | 554 | 553 | 572 | 569 |
| Preg [11,12] | $^{18}O_2$ | 1074 | 1074 | 764 | 764 | 738 | 733 | 506 | 506 | 527 | 527 | 545 | 541 |
| CYP17A1 | $^{16}O_2$ | 1135 | 1136 | 796 | 796 | N.O. | N.O. | 526 | 526 | 546 | 546 | N.O. | N.O. |
| 17-OHPreg | $^{18}O_2$ | 1070 | 1071 | 758 | 758 | N.O. | N.O. | 497 | 497 | 522 | 522 | N.O. | N.O. |
| [11,12] | | | | | | | | | | | | | |

1- requires special care in acquiring RR spectra to Avoid unintentional annealing.

Table 2. Table of abbreviations.

| Abbreviation | Explanation |
|---|---|
| CYP119 | Cytochrome P450 119 |
| CYP101/P450cam | Cytochrome P450 101/Cytochrome P450cam |
| CYP17 | Cytochrome P450 17A1 |
| H/D Shift | Hydrogen/deuterium Shift |
| LA | Lauric acid |
| RR | Resonance Raman |
| Rz | Reinheitszahl ratio |
| v(O—O) | Oxygen-Oxygen stretching mode |
| v(Fe—O) | Iron-Oxygen stretching mode |
| Cam | Camphor |
| N.O. | Not observed |

## 4. Conclusions

This work presents an especially effective approach to study the reactive catalytic intermediates of the thermostable CYP119 with LA bound by means of coupling cryoradiolysis and resonance Raman spectroscopy. The dioxygen adduct was shown to possess two structural isomers, an H-bonded form exhibiting the *v*(O—O) mode at 1130 $cm^{-1}$ and a non-H-bonded conformer at 1139 $cm^{-1}$, both conformers exhibiting their v(Fe—O) modes near 534–535 $cm^{-1}$. The peroxo-CYP119 species produced by radiolytic reduction of oxy-CYP119 exhibits a v(Fe—O) mode at 547 $cm^{-1}$ and its v(O—O) mode at 781 $cm^{-1}$, exhibiting no shift in $D_2O$ buffer, consistent with the assignment to the peroxo-intermediate. The v(Fe—O) mode of the hydroperoxo-CYP119 intermediate occurs at 569 $cm^{-1}$, while the v(O—O) mode is observed at 772 $cm^{-1}$, exhibiting a 5–6 $cm^{-1}$ shift to lower frequencies in $D_2O$, the relative positioning and H/D shifts being entirely consistent with data acquired for the hydroperoxo-intermediates seen for other P450s (see Table 1). These results for CYP119 are consistent with those obtained for other cytochromes P450 upon conversion of oxy- to peroxo- to hydroperoxo- intermediates; i.e., addition of an electron to the ferric superoxide species leads to weaker O—O and stronger Fe—O linkages, with protonation at the terminal oxygen of the Fe-O-O fragment of the peroxo-species increasing the strength of the Fe—O linkage with further weakening of the O—O bond.

## Acknowledgements

This work was supported by a grant from the National Science Foundation (NSF MCB 0951110 to JRK) and the National Institutes of Health (GM125303 to JRK). We greatly appreciate the help of Dr. Jay A. LaVerne while using the $^{60}Co$ source at the Notre Dame Radiation Laboratory (Notre Dame University, IN), which is a facility of the U.S. Department of Energy, Office of basic energy Sciences. J.R.K. gratefully acknowledges the friendship and work of Jim Terner as a valuable source of inspiration and guidance in his own work.

## Declaration of competing interest

None.

## References

[1] A. Sigel, H. Sigel, R.K.O. Sigel (Eds.), The Ubiquitous Roles of Cytochrome P450 Proteins. Metal Ions in Life Sciences, vol 3, John Wiley & Sons, Ltd (2007)

[2] P.R. Ortiz de Montellano (Ed.), Cytochrome P450: Structure, Mechanism, and Biochemistry (4th edition), Springer, Switzerland (2015)

[3] T.L. Poulos. Chem. Rev., 114 (2014), pp. 3919-3962
[4] E.G. Hrycay, S.M. Bandiera. Monooxygenase, Peroxidase and Peroxygenase Properties and Reaction Mechanisms of Cytochrome P450 Enzymes. Springer International Publishing, Switzerland (2015)
[5] X. Huang, J.T. Groves. Chem. Rev., 118 (2018), pp. 2491-2553
[6] R.L. Symons, M.C.R. Peterson. Proc., Proc. R. Soc. London, Ser. B, 201 (1978), pp. 285-300
[7] R. Kappl, M. Höhn-Berlage, J. Hüttermann, N. Bartlett, M.C.R. Symons. Elect, Biochim. Biophys. Acta (BBA)/Protein Struct. Mol., 827 (1985), pp. 327-343
[8] R. Davydov, B.M. Hoffman. Arch. Biochem. Biophys., 507 (2011), pp. 36-43
[9] I. Denisov, T. Makris, S. Sligar. Methods Enzymol., 357 (2002), pp. 103-115
[10] I. Denisov, Y. Grinkova, S. Sligar. Methods Mol. Biol., 875 (2012), pp. 375-391
[11] M. Gregory, P.J. Mak, S.G. Sligar, J.R. Kincaid. Angew. Chem. Int. Ed., 52 (2013), pp. 5342-5345
[12] P.J. Mak, M.C. Gregory, I.G. Denisov, S.G. Sligar, J.R. Kincaid. Proc. Natl. Acad. Sci. U. S. A., 112 (2015), pp. 15856-15861
[13] P.J. Mak, R. Duggal, I.G. Denisov, M.C. Gregory, S.G. Sligar, J.R. Kincaid. J. Am. Chem. Soc., 140 (2018), pp. 7324-7331
[14] I.G. Denisov, P.J. Mak, T.M. Makris, S.G. Sligar, J.R. Kincaid. J. Phys. Chem. A, 112 (2008), pp. 13172-13179
[15] P.J. Mak, I.G. Denisov. Biochim. Biophys. Acta, Proteins Proteomics, 1866 (2018), pp. 178-204
[16] L.R. Brock, T.D. Brock, K.M. Belly, R.T. Weiss. Arch. Mikrobiol., 84 (1972), pp. 54-68
[17] M. De Rosa, A. Gambacorta, J.D. Bu'lock. J. Gen. Microbiol., 86 (1975), pp. 156-164
[18] M.A. McLean, S.A. Maves, K.E. Weiss, S. Krepich, S.G. Sligar. Biochem. Biophys. Res. Commun., 252 (1998), pp. 166-172
[19] Y.R. Lim, C.Y. Eun, H.G. Park, S. Han, J.S. Han, K.S. Cho, Y.J. Chun, D. Kim. J. Microbiol. Biotechnol., 20 (2010), pp. 574-578
[20] L.S. Koo, C.E. Immoos, M.S. Cohen, P.J. Farmer, P.R. Ortiz de Montellano. J. Am. Chem. Soc., 124 (2002), pp. 5684-5691
[21] I.G. Denisov, S.C. Hung, K.E. Weiss, M.A. McLean, Y. Shiro, S.Y. Park, P.M. Champion, S.G. Sligar. J. Inorg. Biochem., 87 (2001), pp. 215-226
[22] J. Rittle, M.T. Green. Science, 330 (2010), pp. 933-937
[23] L.S. Koo, R.A. Tschirret-Guth, W.E. Straub, P. Moënne-Loccoz, T.M. Loehr, P.R. Ortiz De Montellano. J. Biol. Chem., 275 (2000), pp. 14112-14123
[24] Z. Su, J.H. Horner, M. Newcomb. Chembiochem, 13 (2012), pp. 2061-2064
[25] Z. Su, J.H. Horner, M. Newcomb. Chem. Eur. J., 25 (2019), pp. 14015-14020
[26] J. Terner, V. Palaniappan, A. Gold, R. Weiss, M.M. Fitzgerald, A.M. Sullivan, C.M. Hosten. J. Inorg. Biochem., 100 (2006), pp. 480-501
[27] C.M. Hosten, A.M. Sullivan, V. Palaniappan, M.M. Fitzgerald, J. Terner. J. Biol. Chem., 269 (1994), pp. 13966-13978
[28] A.J. Sitter, C.M. Reczek, J. Terner. Biochim. Biophys. Acta Protein Struct. Mol. Enzymol., 828 (1985), pp. 229-235
[29] J.R. Kincaid. Porphyr. Handb. Academic Press, New York (2000), pp. 225-291
[30] P.J. Mak, R. Kadish. K.M. Smith, K. Guilard (Eds.), Porphyr. Handb., Sci, vol 42 (2016), p. 372
[31] V. Palaniappan, J. Terner. J. Biol. Chem., 264 (1989), pp. 16046-16053
[32] J.R. Kincaid, Y. Zheng, J. Al-Mustafa, K. Czarnecki. J. Biol. Chem., 271 (1996), pp. 28805-28811
[33] M. Ibrahim, I.G. Denisov, T.M. Makris, A. James R. Kincaid, Stephen G. Sligar, J.R. Kincaid, S.G. Sligar. J. Am. Chem. Soc., 125 (2003), pp. 13714-13718
[34] J.K. Yano, L.S. Koo, D.J. Schuller, H. Li, P.R. Ortiz De Montellano, T.L. Poulos. J. Biol. Chem., 275 (2000), pp. 31086-31092
[35] E. Mendelovici, R.L. Frost, T. Kloprogge. J. Raman Spectrosc., 31 (2000), pp. 1121-1126
[36] A. Mudalige, J.E. Pemberton. Vib. Spectrosc., 45 (2007), pp. 27-35
[37] M.E. Manyumwa. Resonance Raman Spectroscopy of Isotopically Labeled Cytochrome P450cam and Low Temperature Measurements. Thesis. Marquette University Graduate School (2005), p. 98

[38] R. Usai. Spectral Characterization of Cytochromes P450 Active Sites Using NMR and Resonance Raman Spectroscopy. Marquette University (2017)
[39] Y. Wang, P.J. Mak, Q. Zhu, J.R. Kincaid. J. Raman Spectrosc., 48 (2017), pp. 180-190
[40] C. Rajani, J.R. Kincaid. J. Am. Chem. Soc., 120 (1998), pp. 7278-7285
[41] E. Podstawka, C. Rajani, J.R. Kincaid, L.M. Proniewicz, Cynthia Rajani, James R. Kincaid. Biopolymers, 57 (2000), pp. 201-207
[42] K. Nakamoto. Infrared and Raman Spectra of Inorganic and Coordination Compounds Part a. (Sixth edition), John Wiley & Sons, Inc (2009)
[43] S. Hu, A. Schneider, J. Kincaid. J. Am. Chem. Soc., 113 (1991), pp. 4815-4822
[44] F. Tani, M. Matsu-Ura, S. Nakayama, M. Ichimura, N. Nakamura, Y. Naruta. J. Am. Chem. Soc., 123 (2001), pp. 1133-1142
[45] T. Sjodin, J.F. Christian, I.D.G. Macdonald, R. Davydov, M. Unno, Stephen G. Sligar, A. Brian M. Hoffman, P.M. Champion. Biochemistry, 40 (2001), pp. 6852-6859
[46] D. Kaluka. Spectral Characterization of Cytochromes P450 Active Site and Catalytic Intermediates. Marquette University (2012)
[47] Piotr J. Mak, Ilia G. Denisov, Doreen Victoria, Thomas M. Makris, Tianjing Deng, S.G. Sligar, J.R. Kincaid. J. Am. Chem. Soc., 129 (2007), pp. 6382-6383
[48] Mohammed Ibrahim, James R. Kincaid. J. Porphyrins Phthalocyanins., 8 (2004), pp. 215-225